Biscyanines Linked by a 1,8-Naphthylene Skeleton: Models of Polymethine Dye Aggregates

Takashi Katoh, Keizo Ogawa, Yoshio Inagaki, and Renji Okazaki*,†

Ashigara Research Laboratories, Fuji Photo Film Co., Ltd., 210 Nakanuma, Minami-ashigara, Kanagawa 250-01

†Department of Chemistry, Graduate School of Science, The University of Tokyo, 7-3-1 Hongo, Bunkyo-ku, Tokyo 113

(Received April 16, 1997)

Biscyanines linked by a 1,8-naphthylene skeleton (**1**), suitable model compounds for a study on polymethine dye aggregates, were prepared. Biscyanines, **1b** and **1c**, having methoxy and chloro substituents on the benzothiazole nuclei, respectively, were identified to be in *syn* conformation based upon X-ray crystallographic analysis and NMR spectroscopy. Their absorption maxima were found to be hypsochromically shifted compared to those of the 1-naphthyl substituted monocyanines (**2**). Only a biscyanine **1e** having negatively charged sulfonato groups on the benzothiazole nuclei showed a bathochromic shift and was found to exist as an *anti* conformer. These spectral shifts were reproduced by the calculations with the INDO/S-CI method and are in agreement with those based upon the molecular exciton theory. The positive shifts of the reduction potentials of **1** compared to those of **2** are explained by the Coulombic and orbital interactions between the two cyanine moieties.

Some polymethine dyes form aggregates in aqueous solution and show distinct changes in the positions and band shape of their spectra compared to the corresponding monomers.[1] Usually, bathochromically and hypsochromically shifted bands are called *J*- and *H*-bands, respectively,[2] and the relationship between chromophore arrangements and spectral shifts of polymethine dye aggregates has been explained in terms of molecular exciton theory.[3]

There is very little direct evidence for the aggregate structures of polymethine dyes in solution and on solid surface. Brickstone-work models have been proposed for structures of polymethine dye aggregates based upon crystallographic analyses of various polymethine dye crystals (Fig. 1).[4] Recently, Maskasky applied polarized fluorescence microscopy to *J*-aggregates of polymethine dyes on silver halide grains and proposed brickstone-work structural models.[5]

In order to clarify the relationships between chromophore arrangements and spectral shifts, model compounds in which more than two chromophores were covalently connected to each other were prepared. Kiprianov prepared biscyanines containing two chromophores connected through a benzene ring with various interchromophoric angles.[6] The spectral shifts of these biscyanines were interpreted by molecular exciton theory.[7] However, these compounds are inappropriate as structural models of polymethine dye aggregates, because the two conjugated chains of chromophores are within the same plane. Muchkalo et al. prepared a biscyanine in which the two chromophores were mutually connected by alkylene chains on the nitrogen atoms of the benzimidazole nuclei.[8] The absorption band hypsochromically shifted compared to the corresponding monocyanine suggested the parallel arrangement of the two chromophores, but the biscyanine exists as a mixture of two isomers in solution due to the flexibility of alkylene chains. Thus the relative orientation of two chromophores remains ambiguous.

Little is known about the energy levels of polymethine dye aggregates. This is probably due to the experimental difficulty in isolating a dye aggregate in which the mode of a chromophore arrangement and the number of constituent molecules are well defined. Lenhard and Hein measured the redox potential of a *J*-aggregate of a cationic polymethine dye on silver halide grains by use of a redox buffer method and showed that the excited states of the *J*-aggregate are ca. 0.30 V lower than those of a monomer.[9] However, the chromophore arrangement and the aggregation number remain unknown.

In view of the fact that very few examples of polymethine dye aggregates with well defined structures are known, lack of suitable model compounds may be responsible for the paucity of experimental evidence for the orbital energy levels of aggregates.

Although the synthesis of a dimer covalently connecting two dye molecules seems to be promising as a model of a polymethine dye aggregate because it provides us with isolable aggregate models having well-defined structures, dimers hitherto prepared have some problems, as mentioned above. Recently, we reported the synthesis of pentamethinestreptocyanine oligomers, in which two or three streptocyanines are covalently linked, and clarified the effect of the relative orientation of chromophores on the redox potentials.[10] We also reported the synthesis of 4,4′-(1,8-naphthylene)bispyridines and related pyridinium compounds which are useful intermediates for polymethine dyes.[11]

In this paper, the synthesis of biscyanines linked by a

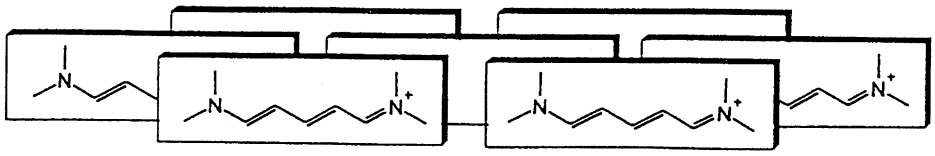

Fig. 1. Brickstone-work model of a polymethine dye aggregate.

1,8-naphthylene skeleton (**1**) and the influence of the chromophore arrangements on their redox potentials are described.

We have designed (1,8-naphthylene)biscyanines suitable for aggregate models in which the molecular planes of polymethine dyes are fixed to make a face-to-face stack. 1,8-Naphthylene skeleton has been used to make a stack of two aromatic rings such as phenyl groups,[12] tolyl groups,[13] substituted tolyl groups,[14] and thienyl groups.[15] 1,8-Di-*m*-tolylnaphthalene has been shown to have two rotational isomers, *syn* and *anti* conformers, where the methyl groups in the tolyl substituent point in the same and opposite directions with respect to the naphthalene plane, respectively.[12] Accordingly, we undertook this study in the expection that the *syn* and the *anti* conformers in (1,8-naphthylene)biscyanines would be suitable models for *H*- and *J*-aggregates, respectively (Fig. 2).

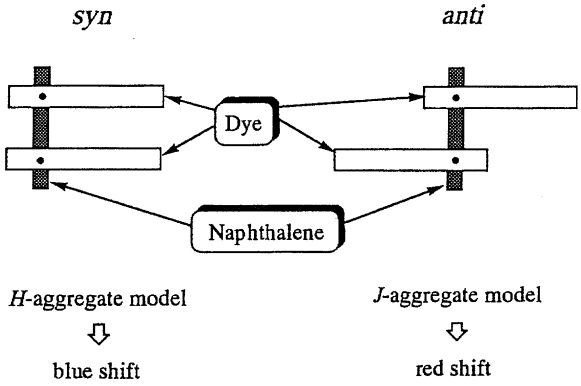

Fig. 2. Two rotational isomers of a (1,8-naphthylene)-biscyanine **1**.

Results and Discussion

Synthesis. (1,8-Naphthylene)biscyanines, **1a**—**1e**, and 1-naphthyl substituted monocyanines, **2a**—**2e**, were prepared by the coupling reactions between 2-methylpyridinium compounds, **3a**[11] and **3b**, and 2-(methylthio)benzothiazolium compounds **4** in moderate yields (Scheme 1).

Structure. The ^{1}H NMR spectrum of the biscyanine **1a** ($R^1 = CH_3$, $R^2 = H$) in DMSO-d_6 at 298 K showed two singlets due to the methine protons in the intensity ratio of 90 : 10. On warming the sample to 343 K, the coalescence of the two signals was observed, suggesting that **1a** exists as a mixture of two rotational isomers. The chemical shifts of methine protons for the major and minor isomers were 0.34 and 0.23 ppm high-field shifted compared to that of the corresponding monomer **2a**, respectively (Table 1). The ^{1}H NMR spectra of biscyanines **1b** ($R^1 = CH_3$, $R^2 = MeO$) and **1c** ($R^1 = CH_3$, $R^2 = Cl$) in DMSO-d_6 at 298 K showed only one singlet for each methine proton and the chemical shifts of methine protons are high-field shifted compared to

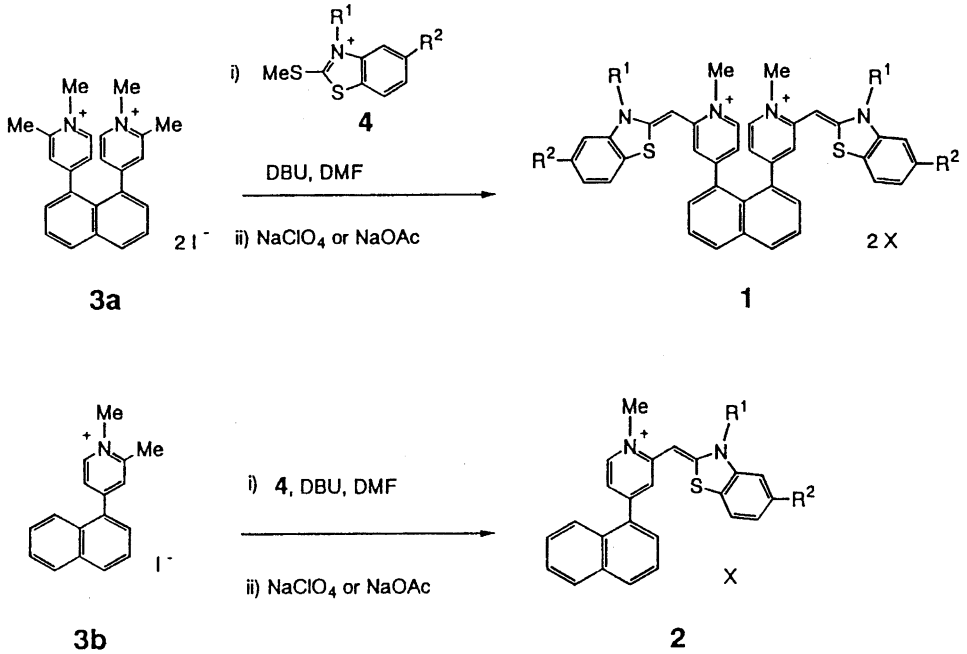

Scheme 1.

Table 1. The Chemical Shifts of Methine Protons, *syn*/*anti* Ratios, Absorption Maxima, and Extinction Coefficients of (1,8-Naphthylene)biscyanines **1** and Monocyanines **2**

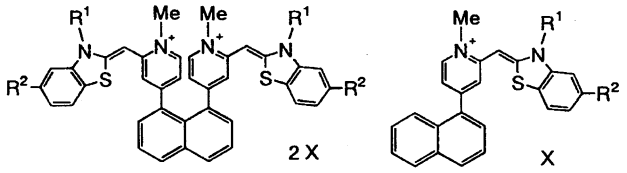

1 **2**

Compounds				Biscyanines **1**			Monocyanines **2**				
	R^1	R^2	X	*syn*/ppm[a]	*anti*/ppm[a]	*syn* : *anti*[b]	λ/nm[c]	$\varepsilon(10^4)$	δ/ppm[d]	λ/nm[c]	$\varepsilon(10^4)$
a	Me	H	ClO_4^-	5.59	5.70	90 : 10	445	5.8	5.93	453	3.4
b	Me	OMe	ClO_4^-	5.64	Not detected	>95 : 5	453	5.0	5.92	461	3.5
c	Me	Cl	ClO_4^-	5.60	Not detected	>95 : 5	442	5.7	5.95	450	3.6
d	$(CH_2)_3SO_3^-$	H	—	5.98	6.14	70 : 30	451	4.4	6.32	454	3.3
e	$(CH_2)_3SO_3^-$	SO_3^-	Na^+	Not detected	6.22	<5 : 95	480	4.9	6.41	454	3.1

a) *Syn* and *anti* stand for chemical shifts of methine protons for *syn* and *anti* conformers in DMSO-d_6 at 298 K, respectively. b) Determined by ^{1}H HMR in DMSO-d_6. c) Absorption maxima in DMSO at 298 K. d) Chemical shifts of the methine protons in DMSO-d_6 at 298 K.

those of the corresponding monocyanines (Table 1).

The ^{1}H NMR spectrum of biscyanine **1d** having 3-sulfonatopropyl groups on nitrogen atoms of the benzothiazole nuclei in DMSO-d_6 at 298 K showed two singlets due to the methine protons in the intensity ratio of 70 : 30. The two peaks shifted to high-field by 0.34 and 0.18 ppm compared to those of the corresponding monocyanine **1d**. In the ROESY (rotating frame nuclear Overhauser effect spectroscopy) spectrum of **1d** in DMSO-d_6, the minor isomers which provided the cross-peaks between the 3- and 5-pyridyl protons were assigned to be an *anti* conformer (Fig. 3).

The major isomers of **1a**—**1c** were assigned to be *syn* conformers by analogy with **1d** where the *syn* conformer showed high-field shifts of the methine protons (Table 1). This result suggests that interaction between the two cyanine moieties of **1a**—**c** is attractive. In order to make an *anti* conformer predominant, further introduction of charge repulsion into **1d** was examined.

Biscyanine **1e** having two sulfonato groups on each one of the benzothiazole nuclei was prepared. The ^{1}H NMR spectrum of **1e** in DMSO-d_6 at 298 K showed only one singlet for the methine protons. Since the methine proton peak is 0.19 ppm high-field shifted than that of **2e** and this shift of **1e** is nearly equal to that of the *anti* conformer of **1d**, **1e** is reasonably considered to exist only in an *anti* conformation in solution. Thus, the charge repulsion between the sulfonato groups in **1e** was proved to be crucial for the preference of an *anti* conformer to a *syn* conformer.

The X-ray crystallographic analysis of **1b** revealed that **1b** exists in a *syn* conformation in solid (Fig. 4) and has the following three structural features:

(1) The methyl groups on the benzothiazole and pyridine nuclei are aligned in the same direction. This configuration in **1b** agrees with that found for the crystal structure of a cyanine monomer **5** (Chart 1).[16]

(2) The splayed-out angle (ϕ) defined by the two pyridine rings is 24°, indicating some repulsion between the two pyridine rings (Fig. 5).

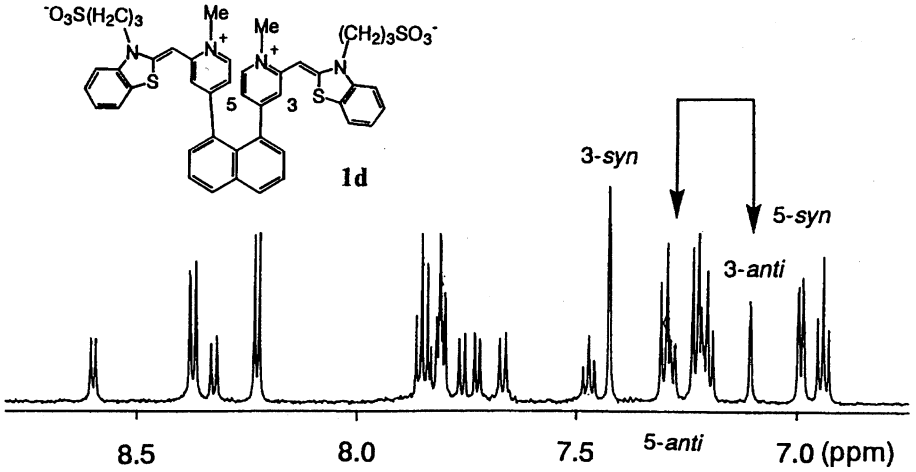

Fig. 3. The ^{1}H NMR spectrum of **1d** in DMSO-d_6 at 298 K. The 3- and 5-pyridyl protons of the *syn* and *anti* conformers are shown. The arrows indicate the cross-peaks of ROESY.

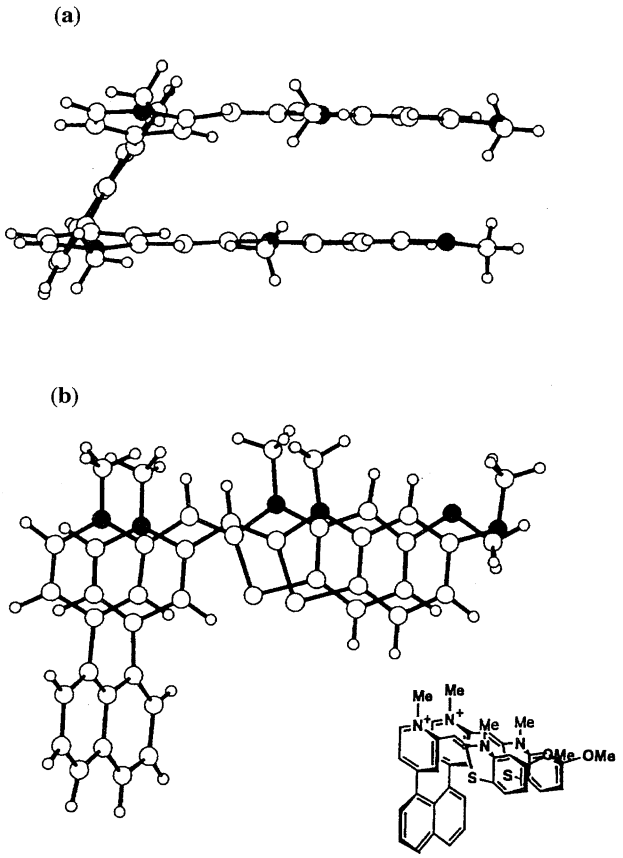

Fig. 4. Molecular structures of the (1,8-naphthylene)-biscyanine **1b**; (a) the top view and (b) the side view.

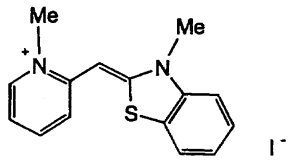

5

Chart 1.

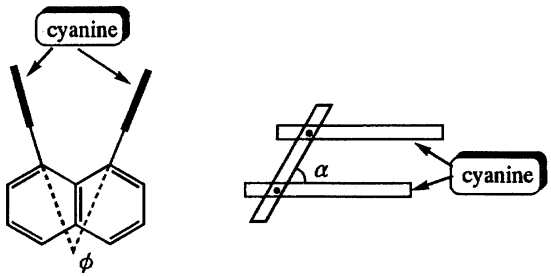

Fig. 5. The splayed-out angle (ϕ) and the slip angle (α) of a (1,8-naphthylene)biscyanine.

(3) The slip angle (α) between the two cyanine moieties is 68° and the distance between the two planes of the cyanine moieties is ca. 3.4 Å, which is a typical value for a face-to-face stack of aromatic rings (Fig. 5).

Absorption Spectra. The absorption bands of the *syn* biscyanines **1b** and **1c** in DMSO are both 8 nm hypsochromically shifted and broader than those of **2b** and **2c**, respectively (Table 1 and Fig. 6a). The crystal absorption maximum (451 nm) of **1b**, which was obtained by a Kramers–Krönig transformation[17] of the reflection spectrum of the single crystal, was nearly equal to that in DMSO (453 nm), confirming the *syn* conformation of **1b** in solution.

The absorption band of the *anti* biscyanine **1e** in DMSO was 26 nm bathochromically shifted compared to that of **2e** (Table 1, Fig. 6b). The half bandwidth of the absorption band of **1e** was larger than that of **2e**. Usually, absorption bands of *J*-aggregates of polymethine dyes are sharper than those of the corresponding monomers.[18] It is interesting that the bathochromically shifted band of the *anti* biscyanine **1e** is rather broad.

Molecular Orbital Calculations. Molecular structures of the biscyanines, **1a** and **1b** (*syn* and *anti*), and the monocyanines, **2a** and **2b**, without counter anions were optimized with the MM2 method.[19] The optimized structure of **1b** (*syn*) with the MM2 method was in better agreement with the result of the X-ray crystallographic analysis than the optimized

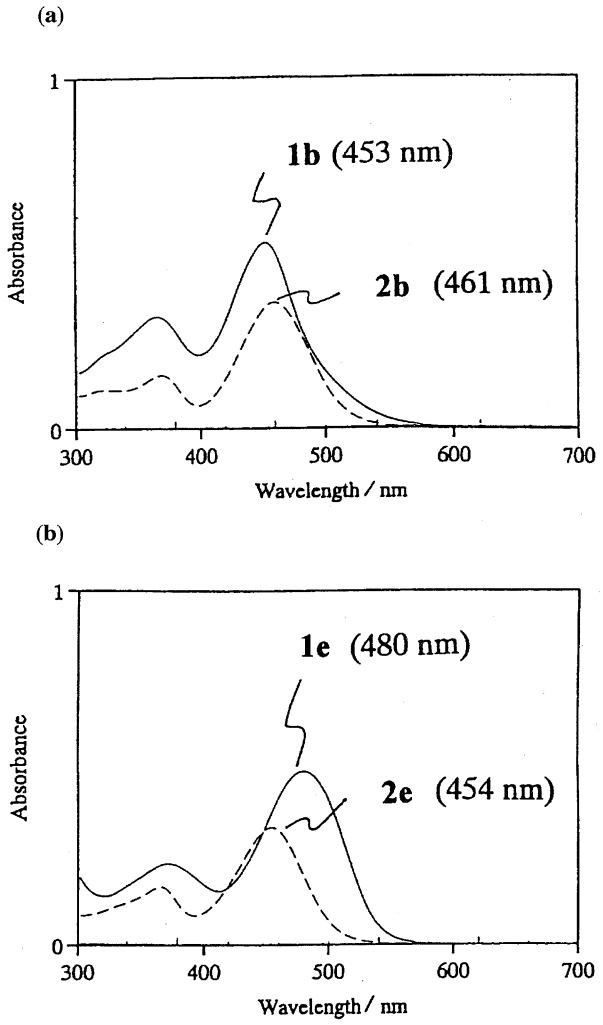

Fig. 6. The absorption spectra in DMSO at 298 K; (a) *syn* biscyanine **1b** and monocyanine **2b**, and (b) *anti* biscyanine **1e** and monocyanine **2e**.

structure with the AM1[20] or the PM3 method.[21] The optimization with the AM1 or the PM3 method gave distorted structures. The calculations with the INDO/S-CI method[22] indicated that the LUMOs of the biscyanines consist of the π orbitals of cyanine dimer moieties and the LUMO levels are not degenerate, due to the orbital interactions between the two cyanine moieties (Table 2). The splitting of LUMO levels (the difference between LUMO and LUMO+1) of **1a** (*anti*) is larger than that of **1a** (*syn*), indicating that the orbital interaction of **1a** (*anti*) is larger than that of **1a** (*syn*). It should be emphasized that the orbital interaction between the two cyanine moieties is not necessarily related to the geometrical overlap between the cyanine moieties. The nodal pattern of the LUMO of **1a** (*syn*) minimizes the orbital interaction between the two cyanine moieties (Fig. 7). The HOMOs of the biscyanines consist of the π orbitals of both cyanine dimer and naphthalene moieties.

The electronic absorption bands calculated with the INDO/S-CI method[22] revealed the hypsochromic shift of the main absorption band for *syn* conformers and the bathochromic shift for *anti* conformers compared to those for the corresponding monocyanines (Table 3). The results of the calculations are in agreement with the observations that *syn* and *anti* biscyanines have hypsochromically and bathochromically shifted absorption bands, respectively. The absorption bands of **1a** (*syn*) consist of intense (417 nm, $f = 1.91$) and weak (492 nm, $f = 0.02$) ones. The main absorption is mainly due to the two transitions of HOMO →LUMO+1 and HOMO-1 →LUMO+1 (HOMO → LUMO stands for a transition from HOMO to LUMO. HOMO-1 means next HOMO), indicating that the main absorption for **1a** (*syn*) is based upon the π–π* transitions of the cyanine dimer moieties, partly accompanied by the naphthalene π – the cyanine dimer π* transitions. On the other hand, the absorption bands for **1a** (*anti*) consist of intense (490 nm, $f = 1.27$) and weak (476 nm, $f = 0.27$) ones and the main absorption is mainly based upon the π–π* transitions of the cyanine dimer moieties (HOMO-1 → LUMO).

Table 2. Orbital Energy Levels of (1,8-Naphthylene)-biscyanines **1a** (*syn* and *anti*) and 1-Naphthyl-monocyanines **2a** Calculated with the INDO/S-CI Method

Compounds[a]	Energy level/eV		
	HOMO	LUMO	LUMO+1
1a (*syn*)	−11.97	−6.47	−6.32
1a (*anti*)	−11.93	−6.35	−6.14
2a	−9.76	−4.06	

a) The MM2 optimized structures without counter anions were used.

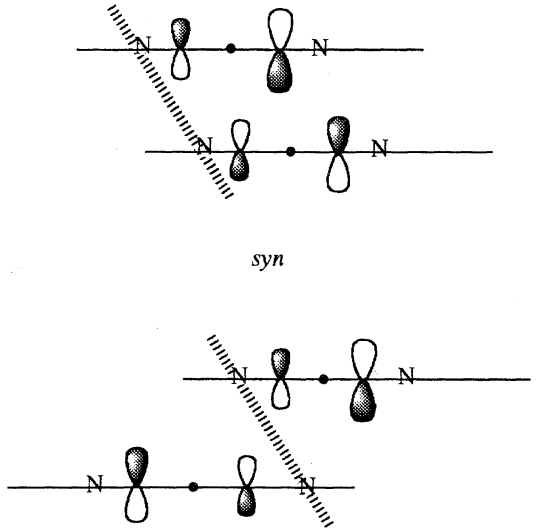

Fig. 7. The nodal patterns of LUMOs of a *syn* and an *anti* conformer of a (1,8-naphthylene)biscyanine. N stands for a nitrogen atom.

In order to estimate the contribution of through-bond interaction, hypothetical dimers **6** (*syn* and *anti*) without a 1,8-naphthylene skeleton, which have the same chromophore arrangements as **1a** (*syn* and *anti*), respectively, were examined (Table 3). The calculation revealed that the degree of the spectral shifts of **6** compared to **5** are nearly equal to those of **1a** compared to **2a**, indicating no through-bond excitonic interaction via a 1,8-naphthylene skeleton.

It is interesting that the weak absorption band for **1a** (*anti*) is bathochromically shifted compared to the absorption for **2a**. When the degree of exciton interaction is small compared to the stabilization of an excited state, based upon Coulombic and van der Waals interaction (ΔH),[23] the forbidden absorption of a *J*-aggregate can be bathochromically shifted compared to that of a monomer (Fig. 8). Accordingly, the calculation on **1a** (*anti*) suggests that ΔH amounts to more than a half of the exciton interaction, although ΔH is often assumed to be small and negligible with respect to exciton interaction.

Fluorescence Spectra. Fluorescence spectra of **1a**, **1b**, **1e**, **2a**, **2b**, and **2e** in DMSO at 298 K were measured (Table 4). It was revealed that the Stokes shift of **1b** is larger than that of **2b**, while the Stokes shift of **1e** is smaller than that of **2e**. These results agree with those expected from the molecular exciton theory. The relative fluorescence intensities of biscyanines **1b** and **1e** are larger than those of monocyanines **2b** and **2e**, respectively. It is interesting that the increased intensity of the hypsochromic biscyanine **1b** is not in agreement with the prediction of the molecular exciton theory that hypsochromic aggregates have weaker fluorescence intensities than monomers.

Redox Potentials. The redox potentials of **1** and **2** measured with polarography revealed that the reduction potentials of the biscyanines **1** are positively shifted compared to those of **2** and the oxidation potentials of **1** are comparable to those of **2** (Fig. 9). The polarograms of **1** indicated one-stage two-electron oxidation and reduction processes.

The positive shifts of reduction potentials of **1** are considered to be caused by both Coulombic and orbital interactions between the two cyanine moieties, since the LUMOs of **1**

Table 3. Absorption Spectra of (1,8-Naphthylene)biscyanines, **1a**, **1b**, and **1e**, 1-Naphthylmonocyanines, **2a**, **2b**, and **2e**, a cyanine **5**, and a Hypothetical Dimers **6** Calculated with the INDO/S-CI Method

Compounds[a]	λ_{max}/nm	f[b]	Transition character[c]
1a (*syn*)	492	0.027	+0.58(H→L)−0.57(H−1→L)+0.42(H−2→L+1)
	417	1.912	−0.33(H→L)−0.53(H→L+1)−0.35(H−1→L) +0.53(H−1→L+1)−0.34(H−2→L)
1a (*anti*)	490	1.27	+0.32(H→L+1)−0.85(H−1→L)−0.33(H−2→L+1)
	476	0.27	+0.50(H→L)+0.70(H−1→L+1)+0.42(H−2→L)
2a	449	0.912	−0.74(H→L)+0.64(H−1→L)
1b (*syn*)	496	0.045	+0.32(H→L)+0.66(H−1→L)−0.37(H−1→L+1) −0.38(H−2→L)−0.33(H−2→L+1)
	432	1.32	+0.65(H→L)+0.62(H−1→L+1)
1b (*anti*)	482	1.27	+0.31(H→L+1)+0.86(H−1→L)−0.32(H−2→L+1)
	467	0.29	+0.50(H→L)+0.70(H−1→L+1)−0.43(H−2→L)
2b	448	0.91	+0.74(H→L)+0.64(H−1→L+1)
1e (*anti*)[d]	457	1.27	+0.87(H→L)−0.40(H−1→L+1)
	443	0.29	+0.75(H→L+1)−0.57(H−1→L)
2e	418	1.12	+0.96(H→L)
6 (*syn*)	498	0.018	+0.69(H→L)−0.40(H→L+1)−0.42(H−1→L) +0.37(H−1→L+1)
	412	1.997	−0.79(H→L+1)+0.47(H−1→L)
6 (*anti*)	475	1.52	+0.89(H→L)−0.40(H−1→L+1)
	460	0.072	−0.79(H→L+1)+0.47(H−1→L)
5	431	1.11	+0.98(H→L)

a) The MM2 optimized structures without counter anions were used. b) Oscillator strength. c) H and L stand for HOMO and LUMO, respectively. d) Calculation of **1e** (*syn*) did not give normal absorption bands.

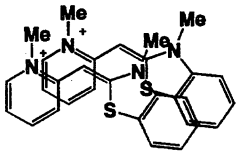

6 (*syn*)

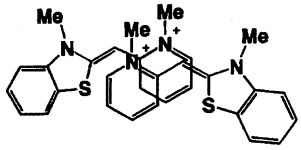

6 (*anti*)

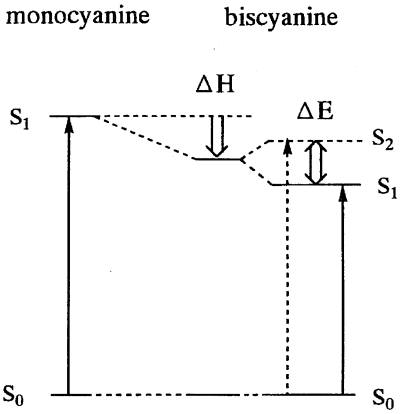

Fig. 8. The schematic energy levels of an *anti* conformer of a (1,8-naphthylene)biscyanine. ΔH stands for Coulombic and van der Waals interaction of an excited state of a biscyanine. ΔE stands for exciton interaction.

consist of the π orbitals of the cyanine dimer moieties. It was reported that Coulombic interaction between neighboring cationic charges and orbital interaction on oligostreptocyanines made the reduction potentials more positive than that of a monomer.[10] The differences in the reduction potentials between **1** and **2** are larger than those between methoxycyanine **1b** and chlorocyanine **1c**, indicating that the influence of aggregation on the reduction potentials is comparable to that of the electronic effects of substituents on the benzothiazole nuclei.

On the other hand, the HOMOs of **1** and **2** mainly consist of the naphthalene π orbitals, so it is not surprising that there is little difference between the oxidation potentials of **1** and **2**.

In order to clarify the effects of relative orientation of chromophores on the redox potentials, the redox potentials of the *syn* biscyanine **1b** and the *anti* biscyanine **1e** were compared (Fig. 10). The positive shift of the reduction potential for **1e** compared to that for **2e** was found to be 0.11 V, which is smaller than that for **1b** (0.19 V). This is understandable, between the distance between the centers of the cyanine moieties in the *anti* conformer (ca. 6.7 Å) is longer than that in the *syn* conformer (ca. 4.0 Å) and hence the overlap between the two cyanine moieties in the *anti* conformer is smaller

Table 4. The Fluorescence Maxima, Stokes Shifts, and Relative Intensities of (1,8-Naphthylene)biscyanines, **1a**, **1b**, and **1e**, and 1-Naphthylmonocyanines, **2a**, **2b**, and **2e**

Compound	Absorpiton	Fluorescence		
	λ_{max}/nm[a)]	λ_{max}/nm[b)]	Stokes shift/cm^{-1}	Relative intensity
1a	445	642	6900	2.844
2a	453	603	5490	1.0 (standard)
1b	453	658	6860	6.38
2b	461	612	5350	2.17
1e	480	616	4600	18.10
2e	454	598	5310	8.75

a) In DMSO at 298 K. b) Fluorescence maxima in DMSO at 298 K with excitation at absorption maxima.

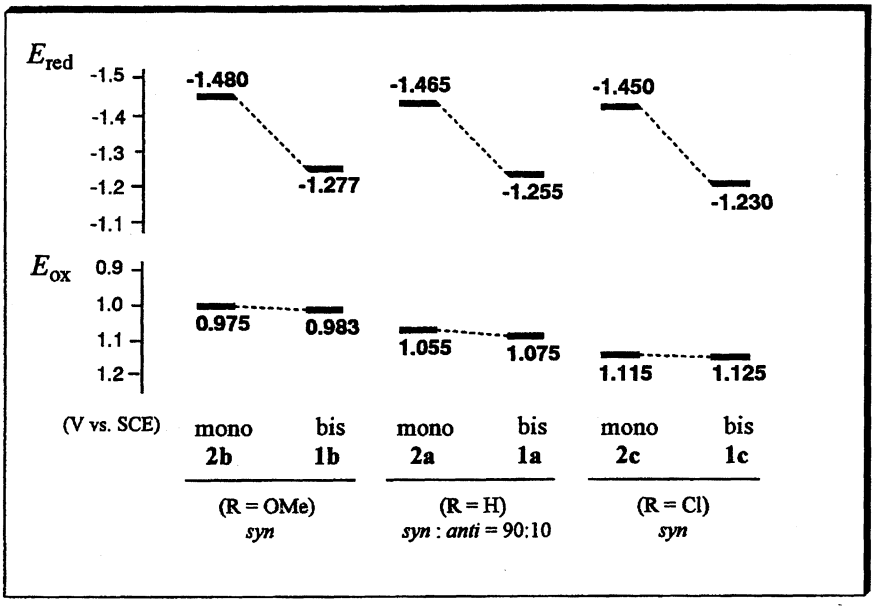

Fig. 9. The redox potentials of biscyanines **1** and monocyanines **2** measured with polarography in CH_3CN with Bu_4NClO_4.

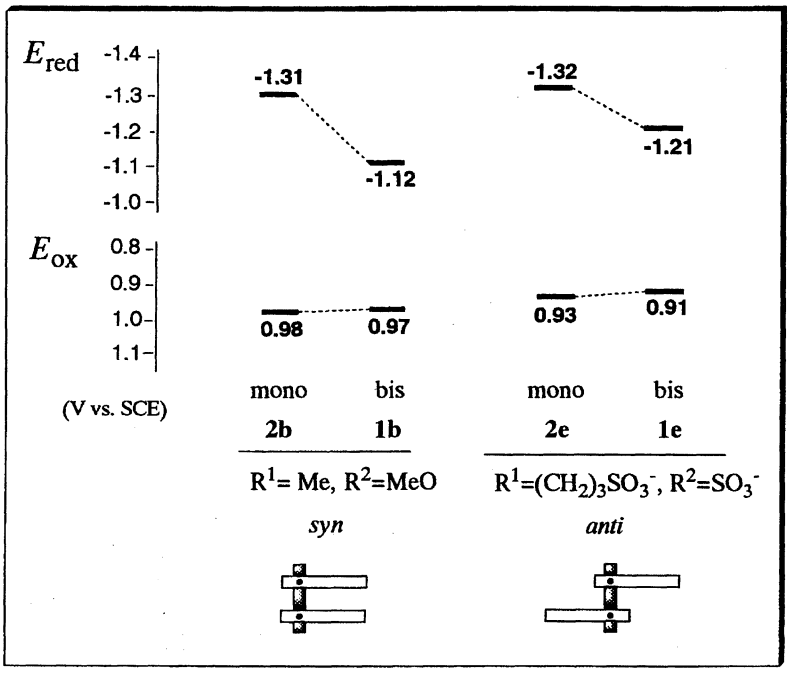

Fig. 10. The redox potentials of *syn* biscyanine **1b** and *anti* biscyanine **1e** measured with polarography in DMSO with Bu_4NClO_4.

than that in the *syn* conformer.

Conclusion. Biscyanines linked by a 1,8-naphthylene skeleton in which chromophore arrangements are suitable to brickstone-work models of polymethine dye aggregates were prepared. The *syn* conformers with slip angles of ca. 68° and the *anti* conformers with slip angles of ca. 29° were found to correspond to *H*- and *J*-aggregate models, respectively, based upon the absorption spectral shifts and the Stokes shifts. The reduction potentials of biscyanines were positively shifted due to the charge and orbital interactions between the two cyanine moieties.

The spectral shifts of absorption bands of dye aggregates are explained by interactions between transition dipoles, while the energy levels of dye aggregates are interpreted in terms of both Coulombic and orbital interaction. It was found that a relative orientation of chromophores in dye aggregates plays an important role to determine energy levels of dye aggregates as well as absorption spectra.

Experimental

Melting points are uncorrected. ^{1}H NMR spectra were determined on a Bruker ARX-300 (300 MHz) or a Bruker AMX-600 (600 MHz) spectrometer, and chemical shifts are quoted in ppm downfield from $SiMe_4$. Infrared spectra were recorded using a JASCO IR-810 spectrometer. UV/vis spectra were recorded on a Shimadzu UV-3100PC spectrometer. FAB-mass spectra were measured by a JEOL DX-303 mass spectrometer. Sephadex LH-20 (Pharmacia Biotech) was used.

A reflection spectrum was measured on a Carl Zeiss microscopic spectrophotometer UMSP50. The reflectivities were converted to absorption coefficients by a Kramers–Krönig transformation. The computation program was based upon the method of Ahrenkiel.[17] Redox potential measurements were carried out on a Yanaco polarographic analyzer P-1100. Reduction and oxidation potentials were measured with mercury and rotating Pt working electrodes, respectively, with a saturated calomel electrode. Acetonitrile and DMSO for electrochemistry were dried over molecular sieves 4 Å.

All MO calculations were performed on a SONY Tektronix CAChe system. Molecular structures were optimized with the MM2 method.[19] The electronic spectra were calculated with the INDO/S-CI method[22] considering 10 configuration interaction levels.

Materials. 4,4′-(1,8-Naphthylene)bis(1,2-dimethylpyridinium) diiodide,[11] 1-methyl-2-(methylthio)benzothiazolium *p*-toluenesufonate,[24] 5-methoxy-3-methyl-2-(methylthio)benzothiazolium *p*-toluenesufonate,[25] 5-chloro-3-methyl-2-(methylthio)benzothiazolium *p*-toluenesufonate,[25] 2-(methylthio)-3-(3-sulfonatopropyl)benzothiazoliumate,[25] and sodium 2-(methylthio)benzothiazole-5-sulfonic acid[26] were prepared by the reported methods.

1,2-Dimethyl-4-(1-naphthyl)pyridinium Iodide (3b). A solution of 2-methyl-4-(1-naphthyl)pyridine[11] (0.15 g, 0.69 mmol) and iodomethane (0.50 g, 3.5 mmol) in CH_3CN (1 ml) was stirred at 40 °C for 3 h. After cooling, the mixture was diluted with acetone (4 ml) and the precipitates were filtered and washed with diethyl ether to give **3b** (0.17 g, 0.47 mmol, 68%) as colorless crystals: Mp 209 °C (decomp); ^{1}H NMR (CD_3OD, 298 K) δ = 2.86 (s, 3H), 4.31 (s, 3H), 7.5—8.2 (m, 9H), 8.90 (d, 1H, J = 8 Hz); IR (KBr) 3520, 1980, 1640, 1560, 1518, 1475, 1395, 1308, 1260, 1200 1156, 1040, 1000, 850, 780 cm^{-1}; MS *m/z* 234 ($M-I^-$). Calcd for $C_{17}H_{16}IN\cdot H_2O$: C, 53.84; H, 4.75; N, 3.69%. Found: C, 53.91; H, 4.48; N, 3.64%.

A Typical Procedure for the Preparation of (1,8-Naphthylene)biscyanines 1. To a solution of **3a**[11] (50 mg, 0.084 mmol) and 2-(methylthio)benzothiazolium *p*-toluenesulfonate (**4**) (0.24 mmol) in DMF (1 ml) was added 1,8-diazabicyclo[5.4.0]undec-7-ene (DBU) (38 mg, 0.25 mmol) and the mixture was stirred at 50 °C for 2 h. After addition of sodium perchlorate (0.1 g, 1.0 mmol) in water (5 ml), the precipitates were filtered off and dissolved in a mixture of dichloromethane and methanol. Then the solvent was removed under reduced pressure until crystals appeared. The precipitates were filtered off and washed with methanol to afford the biscyanines **1**.

4,4′-(1,8-Naphthylene)bis{1-methyl-[2-(3-methylbenzothiazol-2(1*H*)-ylidene)methyl]pyridinium} Diperchlorate (1a): Yield 64%, yellow crystals, mp above 300 °C; λ_{max} (DMSO) 445 nm (ε = 58200); ^{1}H NMR (DMSO-d_6, 298 K) *syn* conformer δ = 3.63 (s, 6H), 4.02 (s, 6H), 5.59 (s, 2H), 6.90 (t, 2H, J = 8 Hz), 6.99 (dd, 2H, J = 2, 7 Hz), 7.1—7.25 (m, 4H), 7.35—7.4 (m, 4H), 7.75—7.90 (m, 4H), 8.21 (d, 2H, J = 7 Hz), 8.39 (d, 2H, J = 8 Hz); IR (KBr) 1638, 1530, 1480, 1380, 1322, 1276, 1221, 1182, 1091, 1020, 880, 820, 744, 716, 621 cm^{-1}; MS *m/z* 733 ($M-ClO_4^-$). Calcd for $C_{22}H_{18}N_2\cdot 0.6H_2O$: C, 57.62; H, 4.11; N, 6.72%. Found: C, 57.59; H, 4.17; N, 6.70%.

4,4′-(1,8-Naphthylene)bis{1-methyl-[2-(5-methoxy-3-methylbenzothiazol-2(1*H*)-ylidene)methyl]pyridinium} Diperchlorate (1b): Yield 27%, yellow crystals: Mp 247 °C (decomp); λ_{max} (DMSO) 453 nm (ε = 49600); ^{1}H NMR (DMSO-d_6, 298 K) δ = 3.71 (s, 6H), 3.80 (s, 6H), 4.07 (s, 6H), 5.64 (s, 2H), 6.95 (dd, 2H, J = 2, 9 Hz), 6.87 (s, 2H), 7.00 (d, 2H, J = 7 Hz), 7.32 (d, 2H, J = 9 Hz), 7.39 (s, 2H), 7.84 (d, 2H, J = 7 Hz), 7.96 (t, 2H, J = 8 Hz), 8.25 (d, 2H, J = 7 Hz), 8.45 (d, 2H, J = 8 Hz); IR (KBr) 3420, 1632, 1539, 1482, 1380, 1340, 1300, 1221, 1179, 1090, 1022, 920, 800, 744, 703, 621 cm^{-1}; MS *m/z* 793 ($M-ClO_4^-$). Calcd for $C_{42}H_{38}Cl_2N_4O_{10}S_2\cdot H_2O$: C, 55.33; H, 4.51; N, 6.14%. Found: C, 55.07; H, 4.39; N, 5.96%

4,4′-(1,8-Naphthylene)bis{1-methyl-[2-(5-chloro-3-methylbenzothiazol-2(1*H*)-ylidene)methyl]pyridinium} Diperchlorate (1c): Yield 44%, yellow crystals: Mp 245—253 °C (decomp); λ_{max} (DMSO) 442 nm (ε = 57400); ^{1}H NMR (DMSO-d_6, 298 K) δ = 3.65 (s, 6H), 4.05 (s, 6H), 5.63 (s, 2H), 6.95—7.08 (m, 4H), 7.3—7.5 (m, 6H), 7.8—7.9 (m, 4H), 8.26 (d, 2H, J = 7 Hz), 8.40 (d, 2H, J = 8 Hz); IR (KBr) 3100, 1632, 1530, 1478, 1421, 1370, 1339, 1330, 1330, 1221, 1182, 1080, 894, 810, 622 cm^{-1}; MS *m/z* 803 ($M-ClO_4^-$). Calcd for $C_{40}H_{32}Cl_4N_4O_8S_2$: C, 53.22; H, 3.57; N, 6.21%. Found: C, 52.91; H, 3.54; N, 6.16%.

4, 4′- (1, 8- Naphthylene)bis[1- methyl- {2- [3- (3- sulfonatopropyl)benzothiazol- 2(1*H*)- ylidene]methyl}pyridinium] (1d): Yield 38%, yellow crystals: Mp 236—250 °C (decomp); λ_{max} (DMSO) 451 nm (ε = 44300); ^{1}H NMR (DMSO-d_6, 298 K) δ = 1.7—1.9 (m, 4H for *syn*), 2.1—2.3 (m, 4H for *anti*), 2.15—2.8 (m, 4H), 4.08 (s, 6H for *anti*), 4.10 (s, 6H for *syn*), 4.3 —4.4 (m, 4H for *syn*), 4.5—4.7 (m, 4H for *anti*), 5.98 (s, 2H for *anti*), 6.14 (s, 2H for *anti*), 6.92 (t, 2H for *syn*, J = 7 Hz), 6.98 (d, 2H for *syn*, J = 6 Hz), 7.10 (s, 2H for *anti*), 7.21 (t, 2H, J = 7 Hz), 7.24 (d, 2H for *syn*, J = 7 Hz), 7.28 (d, 2H for *anti*, J = 7 Hz), 7.32 (d, 2H for *syn*, J = 7 Hz), 7.43 (s, 2H for *syn*), 7.48 (t, 2H for *anti*, J = 7 Hz), 7.67 (d, 2H for *anti*, J = 7 Hz), 7.72 (d, 2H for *anti*, J = 7 Hz), 7.76 (d, 2H for *anti*, J = 7 Hz), 8.21 (d, 2H for *syn*, J = 6 Hz), 8.33 (d, 2H for *anti*, J = 7 Hz), 8.38 (d, 2H for *syn*, J = 7 Hz), 8.60 (d, 2H for *anti*, J = 7 Hz); IR (KBr) 3400, 1638, 1536, 1470, 1390, 1330, 1220, 1180, 1040 cm^{-1}; MS *m/z* 850 ($M+H^+$). Calcd for $C_{44}H_{40}N_4O_6S_4\cdot 1.5H_20$: C, 60.32; H, 4.95; N, 6.33%. Found: C, 60.12; H, 4.99; N, 6.12%.

Preparation of Disodium 4,4′-(1,8-Naphthylene)bis[1-methyl-{2-[3-(3-sulfonatopropyl)benzothiazol-2(1*H*)-ylidene]meth-

yl}pyridinium-5-sulfonate] (1e). To an *N,N*-dimethylacetamide solution (1 ml) of sodium 2-(methylthio)benzothiazole-5-sulfonic acid[26] (0.50 g, 1.8 mmol) was added 1,3-propanesultone (0.50 g, 4.1 mmol) at room temperature and the solution was stirred at 140 °C for 8 h. After addition of ethyl acetate, the precipitates were filtered off and washed with acetone to afford crude sodium 2-(methylthio)-3-(3-sulfonatopropyl)benzothiazolium-5-sulfonate (**4e**) (0.82 g). To a DMF solution (4 ml) of the crude **4e** (0.20 g) and **3a** (0.10 g, 0.18 mmol) was added DBU (0.10 g) at room temperature and the solution was stirred at 60 °C for 1 h. After addition of acetone (5 ml), the precipitates were filtered off and were dissolved in an aqueous methanol solution of sodium acetate (0.1 g, 1.0 mmol). Repeated purification by Sephadex column chromatography using methanol : H_2O (9 : 1) as eluent to afford **1e** (18 mg, 0.017 mmol, 9%) as yellow crystals: Mp above 300 °C; λ_{max} (DMSO) 480 nm (ε = 49200); ^{1}H NMR (DMSO-d_6, 298 K) δ = 2.1—2.3 (m, 4H), 2.8—3.0 (m, 4H), 4.13 (s, 6H), 4.5—4.8 (m, 4H), 6.22 (s, 2H), 7.11 (d, 2H, J = 1 Hz), 7.30 (dd, 2H, J = 1, 7 Hz), 7.43 (d, 2H, J = 9 Hz), 7.65—7.75 (m, 6H), 7.81 (t, 2H, J = 9 Hz), 8.31 (d, 2H, J = 9 Hz), 8.67 (d, 2H, J = 7 Hz); IR (KBr) 3450, 1630, 1520, 1420, 1368, 1320, 1280, 1180, 1105, 1036, 928, 820, 660, 540 cm^{-1}; MS Found: *m/z* 1029.0641. Calcd for $C_{44}H_{38}O_{12}N_4Na_1S_6$: (M − Na^+), 1029.0708.

A Typical Procedure of the Preparation of 1-Naphthylmonocyanines 2. To a solution of **3b** (200 mg, 0.55 mmol) and **6** (0.68 mmol) in acetonitrile (5 ml) was added DBU (120 mg, 0.79 mmol) and the mixture was stirred at 50 °C for 1 h. After addition of sodium perchlorate (0.3 g, 3.0 mmol) in water (10 ml) and methanol (5 ml), the precipitates were filtered off and dissolved in a mixture of dichloromethane and methanol. Then the solvent was removed under reduced pressure until crystals appeared. The precipitates were filtered off and washed with ethanol to afford the monocyanines **2**.

1-Methyl-4-(1-naphthyl)-2-[(3-methylbenzothiazol-2(1*H*)-ylidene)methyl]pyridinium Perchlorate (2a): Yield 46%, yellow crystals: Mp 268—271 °C (decomp); λ_{max} (DMSO) 453 nm (ε = 34200); ^{1}H NMR (DMSO-d_6, 298 K) δ = 3.82 (s, 3H), 4.16 (s, 3H), 5.93 (s, 1H), 7.26 (t, 1H, J = 8 Hz), 7.42 (d, 1H, J = 7 Hz), 7.50 (t, 1H, J = 8 Hz), 7.58—7.80 (m, 5H),7.87 (d, 1H, J = 8 Hz), 7.91 (s, 1H), 7.92—8.00 (m, 1H), 8.10—8.20 (m, 2H), 8.64 (d, 1H, J = 7 Hz); IR (KBr) 1632, 1538, 1480, 1380, 1332, 1298, 1283, 1221, 1190, 1152, 1090, 1020, 849, 802, 741, 718, 622 cm^{-1}; MS *m/z* 381 (M − ClO_4^-). Calcd for $C_{25}H_{21}ClN_2O_4S$: C, 62.43; H, 4.40; N, 5.83%. Found: C, 62.41; H, 4.42; N, 5.77%.

1-Methyl-4-(1-naphthyl)-2-[(5-methoxy-3-methylbenzothiazol-2(1*H*)-ylidene)methyl]pyridinium Perchlorate (2b): Yield 33%, yellow crystals: Mp 275—280 °C (decomp); λ_{max} (DMSO) 461 nm (ε = 35100); ^{1}H NMR (DMSO-d_6, 298 K) δ = 3.82 (s, 3H), 3.85 (s, 3H), 4.14 (s, 3H), 5.92 (s, 1H), 6.88 (d, 1H, J = 9 Hz), 7.23 (s, 1H), 7.39 (d, 1H, J = 7 Hz), 7.60—7.80 (m, 5H), 7.86 (s, 1H), 7.90—7.95 (m, 1H), 8.10—8.20 (m, 2H), 8.62 (d, 1H, J = 6 Hz); IR (KBr) 1630, 1524, 1442, 1372, 1341, 1301, 1272, 1221, 1182, 1142, 1092, 1022, 938, 800, 708, 621 cm^{-1}; MS *m/z* 411 (M − ClO_4^-). Calcd for $C_{26}H_{23}ClN_2O_5S$: C, 61.11; H, 4.54; N, 5.48%. Found: C, 60.92; H, 4.45; N, 5.45%.

1-Methyl-4-(1-naphthyl)-2-[(5-chloro-3-methylbenzothiazol-2(1*H*)-ylidene)methyl]pyridinium Perchlorate (2c): Yield 29%, yellow crystals: Mp 280—288 °C (decomp); λ_{max} (DMSO) 450 nm (ε = 36500); ^{1}H NMR (DMSO-d_6, 298 K) δ = 3.79 (s, 3H), 4.17 (s, 3H), 5.95 (s, 1H), 7.29 (d, 1H, J = 8 Hz), 7.49 (d, 1H, J = 7 Hz), 7.70—7.80 (m, 5H), 7.82 (d, 1H, J = 8 Hz), 7.90—8.00 (m, 2H), 8.10—8.25 (m, 2H), 8.68 (d, 1H, J = 7 Hz); IR (KBr) 3100, 1638, 1530, 1480, 1461, 1421, 1374, 1339, 1300, 1272, 1222, 1190, 1150, 1090, 936, 880, 803, 780, 720, 621, 598 cm^{-1}; MS *m/z* 415 (M − ClO_4^-). Calcd for $C_{25}H_{20}Cl_2N_2O_4S$: C, 58.26; H, 3.91; N, 5.44%. Found: C, 58.00; H, 3.83; N, 5.37%.

1-Methyl-4-(1-naphthyl)-2-{[3-(3-sulfonatopropyl)benzothiazol-2(1*H*)-ylidene]methyl}pyridinium (2d): Yield 59%, yellow crystals: Mp above 300 °C; λ_{max} (DMSO) 454 nm (ε = 32800); ^{1}H NMR (DMSO-d_6, 298 K) δ = 2.0—2.2 (m, 2H), 2.6—2.8 (m, 2H), 4.21 (s, 3H), 4.6—4.7 (m, 2H), 6.32 (s, 1H), 7.25 (t, 1H, J = 8 Hz), 7.38 (dd, 1H, J = 1, 7 Hz), 7.49 (t, 1H, J = 8 Hz), 7.65—7.75 (m, 5H), 7.82 (d, 1H, J = 8 Hz), 7.90 (d, 1H, J = 1 Hz), 7.95—8.00 (m, 1H), 8.10—8.20 (m, 2H), 8.62 (d, 1H, J = 7 Hz); IR (KBr) 3420, 1636, 1530, 1478, 1390, 1330, 1298, 1272, 1218, 1178, 1040, 860, 802, 750, 722 cm^{-1}; MS *m/z* 489 (M + H^+). Calcd for $C_{27}H_{24}N_2O_3S_2 \cdot H_2O$: C, 64.01; H, 5.17; N, 5.53%. Found: C, 63.78; H, 4.97; N, 5.78%.

Preparation of Sodium 1-Methyl-4-(1-naphthyl)-2-{[3-(3-sulfonatopropyl)benzothiazol- 2(1*H*)- ylidene]methyl}pyridinium-5-sulfonate (2e). To a DMF solution (4 ml) of **3b** (0.10 g, 0.18 mmol) and crude **4e** (0.20 g), which was prepared by above-mentioned procedure for the preparation of **1e**, was added DBU (0.10 g, 0.65 mmol) at room temperature, and the solution was stirred at 50 °C for 1 h. After addition of acetone, the precipitates were filtered off and were dissolved in aqueous methanol solution of sodium acetate (0.1 g, 1.0 mmol). Repeated purification by Sephadex column chromatography using methanol–H_2O (9 : 1) as eluent to afford **2e** (23 mg, 0.038 mmol, 22%) as yellow crystals: Mp 265—272 °C (decomp); λ_{max} (DMSO) 454 nm (ε = 31200); ^{1}H NMR (DMSO-d_6, 298 K) δ = 2.0—2.2 (m, 2H), 2.8—2.9 (m, 2H), 4.23 (s, 3H), 4.5—4.7 (m, 2H), 6.41 (s, 1H), 7.41 (d, 1H, J = 6.0 Hz), 7.46 (d, 1H, J = 8.8 Hz), 7.60—7.80 (m, 6H), 7.90 (s, 1H), 7.92—8.00 (m, 1H), 8.10—8.20 (m, 2H), 8.63 (d, 1H, J = 6.0 Hz); IR (KBr) 3450, 1638, 1538, 1420, 1370, 1200, 1112, 1042, 804, 670 cm^{-1}. MS Found: *m/z* 591.0681. Calcd for $C_{27}H_{24}N_2NaO_6S_3 + H^+$: (M + H^+), 591.0694.

X-Ray Crystallographic Analysis of 1b.[27] A single crystal of biscyanine **1b** was obtained by recrystallization from methanol. The X-ray diffraction data collection was performed on a Rigaku AFC-5R diffractometer using monochromated Cu $K\alpha$ radiation and a scan width of (1.78 + 0.3 tan θ)° within 2 θ < 120.3°. The structure was solved by direct methods (MITHRIL 90)[28] and expanding using Fourier techniques. The final cycle of full-matrix least-squares refinement was converged to the final R factor of 0.111.

Crystal Data: Monoclinic, $P2_1/c$, a = 11.118(4), b = 15.697(3), c = 24.627(3) Å, β = 100.35(2)°, Z = 4, D_{calc} = 1.448 g dm^{-3}; μ(Cu $K\alpha$) = 28.72 cm^{-1}, $F(000)$ = 1912, T = 296 K, Total unique data 6569, No. of observations [$I \geqq 3\sigma(I)$] 1959, R = 0.111, R_w = 0.081.

References

1) D. Möbius, *Adv. Mater.*, **7**, 437 (1995); N. Tyutyulkov, J. Fabian, A. Mehlohorn, F. Dietz, and A. Tadjer, "Polymethine Dyes," St. Kliment Ohridski University Press, Sofia (1991); A. H. Herz, *Photogr. Sci. Eng.*, **18**, 323 (1974); T. Tani, "Photographic Sensitivity," Oxford University Press, New York (1995), Chap. 5, pp. 111—164; D. M. Sturmer and D. W. Heseltine, "The Theory of the Photographic Process," 4th ed, ed by T. H. James, McMillan Publ. Co., New York (1977), Chap. 8, pp. 194—234; P. B. Gilman, *Pure Appl. Chem.*, **49**, 357 (1977); W. West, *Photogr. Sci. Eng.*, **18**, 35 (1974).

2) E. E. Jelly, *Nature*, **138**, 1009 (1936); G. Scheibe, *Angew. Chem.*, **49**, 563 (1936).

3) E. G. McRae and M. Kasha, *J. Chem. Phys.*, **28**, 721 (1958); M. Kasha, H. R. Rawis, and M. A. El-Bayoumi, *Pure Appl. Chem.*, **11**, 371 (1965); G. S. Levinson, W. T. Simpson, and W. Curtius, *J. Am. Chem. Soc.*, **79**, 4314 (1957); K. Norland, A. Ames, and T. Taylor, *Photogr. Sci. Eng.*, **14**, 295 (1970).

4) E. S. Emerson, M. A. Conlin, A. E. Rosenoff, K. S. Norland, H. Rodriguez, D. Chin, and G. R. Bird, *J. Phys. Chem.*, **71**, 2396 (1967); D. L. Smith, *Photogr. Sci. Eng.*, **16**, 329 (1972); S. Makio, N. Kanamaru, and J. Tanaka, *Bull. Chem. Soc. Jpn.*, **53**, 3120 (1980).

5) J. E. Maskasky, *Langmuir*, **7**, 407 (1991); J. E. Maskasky, *J. Imaging Sci.*, **35**, 29 (1991).

6) A. I. Kiprianov, *Uspekhi Khim.*, **40**, 1283 (1971).

7) G. G. Dyadyusha, A. M. Kolesnikov, and A. D. Kachkovskii, *Dyes Pigm.*, **10**, 111 (1989).

8) I. L. Mushkalo, G. G. Dyadyusha, L. S. Turova, and M. Y. Kornilov, *Tetrahedron Lett.*, **21**, 2977 (1980).

9) J. R. Lenhard and B. R. Hein, *J. Phys. Chem.*, **100**, 17287 (1996).

10) T. Katoh, Y. Inagaki, and R. Okazaki, *Bull. Chem. Soc. Jpn.*, **70**, 2279 (1997).

11) T. Katoh, Y. Inagaki, K. Ogawa, and R. Okazaki, *Tetrahedron*, **22**, 3557 (1997).

12) H. O. House, D. G. Koepsell, and W. J. Campbell, *J. Org. Chem.*, **37**, 1003 (1972); R. Tsuji, K. Komatsu, K. Takeuchi, M. Shiro, S. Cohen, and M. Rabinovitz, *J. Phys. Org. Chem.*, **6**, 435 (1993).

13) F. Vögtle and R. Wingen, *Tetrahedron Lett.*, **17**, 1459 (1978).

14) F. Cozzi, M. Cinquini, R. Annuziata, T. Dwyer, and J. S. Siegel, *J. Am. Chem. Soc.*, **114**, 5729 (1992); F. Cozzi, M. Cinquini, R. Annuziata, and J. S. Siegel, *J. Am. Chem. Soc.*, **115**, 5330 (1993); F. Cozzi, F. Ponzini, R. Annunziata, M. Cinquini, and J. S. Siegel, *Angew. Chem., Int. Ed. Engl.*, **34**, 1019 (1995).

15) M. Kuroda, J. Nakayama, M. Hoshino, N. Furusho, T. Kawata, and S. Ohba, *Tetrahedron*, **18**, 3735 (1993).

16) G. Wu, X-f. Zhou, K. Vanhulle, A. T. H. Lenstra, and H. J. Geise, *J. Imaging Sci. Technol.*, **39**, 253 (1995).

17) R. K. Ahrenkiel, *J. Opt. Soc. Am.*, **61**, 165 (1971).

18) E. W. Knapp, P. O. J. Scherer, and S. F. Fischer, *Chem. Phys. Lett.*, **111**, 481 (1984); H. Fidder, J. Knoester, and D. A. Wiersma, *J. Chem. Phys.*, **95**, 7880 (1991); K. Ya. Burshtein, A. A. Bagatur'yants, and M. V. Alfimov, *Chem. Phys. Lett.*, **239**, 195 (1995).

19) N. L. Allinger, *J. Am. Chem. Soc.*, **99**, 8127 (1985).

20) M. J. S. Dewer, E. G. Zoebisch, E. F. Healy, and J. J. P. Stewart, *J. Am. Chem. Soc.*, **107**, 3902 (1985).

21) J. J. P. Stewart, *J. Comput. Chem.*, **10**, 209 (1989).

22) J. Ridley and M. Zerner, *Theor. Chim. Acta (Berlin)*, **32**, 111 (1973).

23) M. S. Gudipati, *J. Phys. Chem.*, **98**, 9750 (1994).

24) D. M. Fabricius and R. J. Le Strange, Eur. Patent, EP 467155.

25) X-f. Zhou, Z-h. Peng, H. J. Geise, B-x. Peng, Z-x. Li, M. Yan, R. Dommisse, R. Carleer, and M. Claeys, *J. Imaging Sci. Technol.*, **39**, 244 (1995).

26) A. Mikawa and T. Shishido, Japan Patent, JP 50-92125o.

27) Full crystal data, atom coordinates, thermal parameters, and bond distances and angles are deposited as Document No. 70035 at the Office of the Editor of Bull. Chem. Soc. Jpn.

28) C. J. Gilmore, "MITHRIL—an integrated direct methods computer program," University of Glasgow, Scotland (1990).